Available online at http://ijim.srbiau.ac.ir/
Int. J. Industrial Mathematics (ISSN 2008-5621)
Vol. 14, No. 3, 2022 Article ID IJIM-1500, 10 pages
DOI: http://dx.doi.org/10.30495/ijim.2022.59473.1500
Research Article

Numerical Study of Two Reaction Mechanisms on Delft Flame III Using Large Eddy Simulation and Conditional Moment Closure Approach

M. Zakyani Roudsari *†

Received Date: 2021-03-06 Revised Date: 2022-01-03 Accepted Date: 2022-05-15

Abstract

A conditional moment closure model is adopted together with a state-of- the-art LES approach to simulate the target flame of the TNF workshop, Delft piloted methane flame III. For modeling the sub-grid scales, the constant Smagorinky model is used in this study. First order conditional moment closure is used to model the turbulence-chemistry interaction. To calculate the conditional velocity and the conditional scalar dissipation, conditional volume averaging with smoothing is used. To study the effect of the chemistry, two different methane reaction mechanisms are used. The first reaction mechanism is the one-step methane chemistry with 4 species and 1 reaction. The second reaction mechanism is the Smooke reaction mechanism which consists of 16 species and 25 reactions. A second order time accurate predictor-corrector method is used for time integration of the Favre filtered Navier-Stokes equations. It is shown that the reaction mechanisms has almost no influence on velocity and scalar fields. However, the temperature field is influenced by using a more complex reaction mechanism.

Keywords : Turbulent Combustion; Large Eddy Simulation; Conditional Moment Closure; Non-premixed Flame; Chemical Reaction Mechanism.

1 Introduction

The simulation of non-premixed turbulent flames remains a significant topic in science and engineering which has many industrial applications. Efforts for modeling these kinds of flames help us to comprehend the nature of turbulence-chemistry interaction. Due to the extremely complex nature of the phenomena involved in this subject, modeling turbulence-chemistry interaction remain a complex task. Turbulence manifests itself through a broad spectrum of time and length scales: from large coherent structure to very small scales thought to be more universal. On the contrary, combustion which is a chemical process can only happen at small scales i.e., molecular scales. These scales are normally considerably smaller than the smallest turbulence time and length scales. Therefore, the interaction between these various scales remains a fascinating topic and modeling this phenomenon remain

*Corresponding author. zakyani@ari.ac.ir, Tel:+98(21)88366035.
†Aerospace Research Institute of Iran, Tehran, Iran.

a challenging subject. Needless to mention that understanding this phenomenon will help to design more efficient engineering devices such as the combustion chamber of the gas turbines, automobile engines, etc. Models proposed to calculate unclosed terms in non-reactive LES are not applicable in reactive flow equations, namely species mass fraction and enthalpy equations. The problem arises when we want to define filtered chemical reaction rate and heat release in terms of filtered species mass fractions and enthalpy in their filtered equations.

The CMC model was initially proposed for RANS turbulence models. E.g., Roomina and Bilger [20] used first order conditional moment closure with $k-\varepsilon$ RANS turbulence model to simulate the Sandia D flame. Other studies with first order CMC in the RANS context can be found in e.g., [6] and [7]. Mastorakos and Bilger [11] used second order CMC to study auto-ignition in turbulent flames. The extension to second order is necessary to adequately capture the auto-ignition phenomenon. Cha et al. [4] and Kronenburg [10] properly used doubly conditional moment approach to simulate extinction and re-ignition in non-premixed flames in the RANS context.

As LES showed promising results in simulation and modeling of non-combustive test cases, turbulent combustion models which have been successfully adopted in RANS simulation adapted for LES. Many experimental flames were simulated using LES and they showed good agreement with the experimental data. Pitsch and Steiner [17] used lagrangian flamelet model to simulate non-premixed methane flame, Sandia flame D. They adopted Dynamic procedure to fine tune the Smagorinsky constant. Branley and Jones [2] used equilibrium chemistry and dynamic Smagorinsky procedure to simulate hydrogen diffusion flame. Sheikhi et al. [21] used scalar filtered mass density function methodology and large eddy simulation to model Sandia flame D. Navarro-Martinez et al. [13] used conditional moment closure approach together with dynamic Smagorinsky procedure to simulate Sandia flame D. Results for the Sydney bluff body burner are presented in [14] using CMC together with the dynamic Smagorinsky model. A comprehensive review of adoption of LES for simulating of combustion systems can be found in [18].

2 Flow Modeling

Applying Favre filter to the Navier-Stokes equations, the final equation reads

$$\frac{\partial \overline{\rho}}{\partial t} + \frac{\partial \overline{\rho}\widetilde{u}_i}{\partial x_i} = 0 \tag{2.1}$$

$$\begin{aligned} &\frac{\partial \overline{\rho}\widetilde{u}_i}{\partial t} + \frac{\partial \overline{\rho}\widetilde{u}_i\widetilde{u}_j}{\partial x_j} = -\frac{\partial \overline{p}}{\partial x_i} \\ &+ \frac{\partial}{\partial x_j}[\overline{\mu}(\frac{\partial \widetilde{u}_i}{\partial x_j} + \frac{\partial \widetilde{u}_j}{\partial x_i} - \frac{2}{3}\delta_{ij}\frac{\partial \widetilde{u}_k}{\partial x_k}) - \tau_{ij}^{sgs}] \end{aligned} \tag{2.2}$$

The Favre filtered mixture fraction equation is given by

$$\begin{aligned} &\frac{\partial \overline{\rho}\widetilde{\xi}}{\partial t} + \frac{\partial \overline{\rho}\widetilde{u}_j\widetilde{\xi}}{\partial x_j} \\ &= \frac{\partial}{\partial x_j}\left(\overline{\rho}\overline{D}\frac{\partial \widetilde{\xi}}{\partial x_j} - \overline{\rho}J_j^{sgs}\right) \end{aligned} \tag{2.3}$$

2.1 Sub-grid scale model

The sub-grid scale (SGS) stress term in the Favre filtered momentum equations can be modeled as

$$\begin{aligned} &\tau_{ij}^{sgs} - \frac{1}{3}\tau_{kk}^{sgs}\delta_{ij} = \\ &- 2\mu_t(\widetilde{S}_{ij} - \frac{1}{3}\widetilde{S}_{mm}\delta_{ij}) \end{aligned} \tag{2.4}$$

To close the Favre filtered mixture fraction equation, sub-grid scale turbulent scalar flux should be modeled. To model the mentioned term a gradient model is used,

$$J_j^{sgs} = -D_t\frac{\partial \widetilde{\xi}}{\partial x_j} \tag{2.5}$$

where D_t is the turbulent diffusivity and is defined as,

$$D_t = \frac{\nu_t}{Sc_t} \tag{2.6}$$

where the dynamic turbulent diffusivity, ν_t, is given by the sub-grid scale model and is computed as,

$$\nu_t = \frac{\mu_t}{\overline{\rho}} \tag{2.7}$$

and Sc_t is the turbulent Schmidt number which is set to 0.7 in this work following [2, 15].

In above equations we need to find the turbulent viscosity, μ_t. Different sub-grid scale proposed to define turbulent viscosity. Constant Smagorinsky [22] is one of the first model proposed to calculate the sub-gird scale term of the momentum equations. Smagorinsky proposed that the turbulent diffusivity can be calculated as

$$\mu_t = \overline{\rho}(C_S\Delta)^2|\widetilde{S}_{ij}| \tag{2.8}$$

$$\widetilde{S}_{ij} = \frac{1}{2}\left(\frac{\partial\widetilde{u}_i}{\partial x_j} + \frac{\partial\widetilde{u}_j}{\partial x_i}\right) \tag{2.9}$$

where C_S is the Smagorinsky constant. Branley and Jones [2] propose $C_S = 0.1$ in their studies. Therefore, $C_S = 0.1$ is used for the Smagorinsky constant in the present work. Δ is the filter width which is given by the cubic root of the local grid cell volume.

2.2 Combustion Modeling

As was mentioned before, the CMC model is used for the simulation of turbulent-chemistry interaction. In the CMC model transport equations for the conditional mass fraction equations are solved in time, physical space and mixture fraction space. Final equations for the conditional species mass fraction and the conditional temperature following Navarro-Martinez et al. [13] take the form

$$\begin{aligned}&\frac{\partial\widetilde{Y_\alpha|\eta}}{\partial t} + \widetilde{u_i|\eta}\frac{\partial\widetilde{Y_\alpha|\eta}}{\partial x_i} = \widetilde{\chi|\eta}\frac{\partial^2\widetilde{Y_\alpha|\eta}}{\partial\eta^2}\\ &+ \frac{\partial}{\partial x_i}(\widetilde{D_t|\eta}\frac{\partial\widetilde{Y_\alpha|\eta}}{\partial x_i}) + \widetilde{W_\alpha|\eta}\end{aligned} \tag{2.10}$$

$$\begin{aligned}&\frac{\partial\widetilde{T|\eta}}{\partial t} + \widetilde{u_i|\eta}\frac{\partial\widetilde{T|\eta}}{\partial x_i} = \widetilde{\chi|\eta}\frac{\partial^2\widetilde{T|\eta}}{\partial\eta^2}\\ &+ \frac{\partial}{\partial x_i}(\widetilde{D_t|\eta}\frac{\partial\widetilde{T|\eta}}{\partial x_i}) + \widetilde{\chi|\eta}[\frac{1}{\widetilde{c_p|\eta}}(\frac{\partial\widetilde{c_p|\eta}}{\partial\eta}\\ &+ \sum_{\alpha=1}^{n}(c_p)_\alpha\frac{\partial\widetilde{Y_\alpha|\eta}}{\partial\eta})]\frac{\partial\widetilde{T|\eta}}{\partial\eta}\\ &+ \frac{1}{\widetilde{c_p|\eta}}\frac{1}{\rho}\widetilde{\frac{\partial p}{\partial t}|\eta} + \frac{\widetilde{W_T|\eta}}{\widetilde{c_p|\eta}}\end{aligned} \tag{2.11}$$

where $\widetilde{Y_\alpha|\eta}$ stands for the Favre conditional filtered mass fraction of species α and $\widetilde{T|\eta}$ stands for the Favre conditional filtered temperature, respectively defined as

$$\widetilde{Y_\alpha|\eta} = \frac{\overline{\rho Y_\alpha|\eta}}{\overline{\rho|\eta}} \tag{2.12}$$

$$\widetilde{T|\eta} = \frac{\overline{\rho T|\eta}}{\overline{\rho|\eta}} \tag{2.13}$$

The term involving the time variation of pressure in the conditional temperature equation is neglected as a low Mach approximation is used in this work. To obtain the conditional velocity, the conditional scalar dissipation rate and the conditional turbulent diffusion, conditional volume averaging of the LES data is used. To obtain unconditional mass fractions and temperature, the conditional values, obtained from solving the conditional equations are integrated with the FDF as

$$\widetilde{\varphi} = \int\widetilde{\varphi|\eta}\widetilde{P}(\eta)d\eta \tag{2.14}$$

As FDF a β-function is used whose shape depends on the first and the second moment of the mixture fraction. The first moment is the filtered mixture fraction for which a transport equation, is solved at every iteration. The second moment is the sub-grid scale variance of the mixture fraction. To find the mixture fraction variance a local equilibrium assumption is used

$$\widetilde{z''^2} = C\Delta^2|\nabla\widetilde{z}|^2 \tag{2.15}$$

Branley and Jones [2] suggest a value equals to 0.1 for C but it is chosen to be 0.09 in this study. The scalar dissipation rate is obtained using a simple equilibrium model [9]

$$\widetilde{\chi} = (\frac{\widetilde{\mu}}{Sc} + \frac{\mu_t}{Sc_t})|\nabla\widetilde{z}|^2 \tag{2.16}$$

where Sc is laminar Schmidt numbers which is 0.7 in this work and $\widetilde{\mu}$ is filtered dynamic viscosity.

3 Numerical Algorithm

3.1 Flow Solver Algorithm

The LES code used for solving the Navier-Stokes equations is an in-house code. The flow equations are solved using the projection method of Chorin [5]. The resulting Poisson equation for the pressure is solved with an alternating line Gauss-Seidel method. To accelerate convergence a multigrid method is used. The convective fluxes are discretized with a second order central scheme for the momentum equation and second order TVD scheme with Van Leer limiter for the mixture fraction equation. A predictor-corrector method [17] is used for time integration of the unsteady Favre filtered Navier-Stokes equations. For completeness the predictor-corrector method used in this study, which is 2nd order accurate in time, is shortly explained.

Predictor Step Using the second order Adams-Bashforth method with variable step size for time integration of the Navier-Stokes equations, the discretized momentum equations read

$$\frac{\widehat{(\overline{\rho}\widetilde{u}_i)^*} - (\overline{\rho}\widetilde{u}_i)^n}{\Delta t^n} = (1+\frac{1}{2}\frac{\Delta t^n}{\Delta t^{n-1}})Res_u^n - (\frac{1}{2}\frac{\Delta t^n}{\Delta t^{n-1}})Res_u^{n-1} \tag{3.17}$$

where Res_u is defined as

$$Res_u = -\frac{\partial \overline{\rho}\widetilde{u}_i\widetilde{u}_j}{\partial x_j} + \frac{\partial}{\partial x_j}((\overline{\mu}+\mu_t)(\frac{\partial \widetilde{u}_i}{\partial x_j}+\frac{\partial \widetilde{u}_j}{\partial x_i}-\frac{2}{3}\frac{\partial \widetilde{u}_k}{\partial x_k})) \tag{3.18}$$

Applying the same method for the mixture fraction equation we have

$$\frac{(\overline{\rho}\widetilde{z})^* - (\overline{\rho}\widetilde{z})^n}{\Delta t^n} = (1+\frac{1}{2}\frac{\Delta t^n}{\Delta t^{n-1}})Res_z^n - (\frac{1}{2}\frac{\Delta t^n}{\Delta t^{n-1}})Res_z^{n-1} \tag{3.19}$$

where Res_z is defined as

$$Res_z = -\frac{\partial \overline{\rho}\widetilde{u}_i\widetilde{z}}{\partial x_i} + \frac{\partial}{\partial x_i}(\overline{\rho}(\overline{D}+D_t)\frac{\partial \widetilde{z}}{\partial x_i}) \tag{3.20}$$

where from the known mixture fraction field the density field is calculated as

$$\widetilde{z}^* = \frac{(\overline{\rho}\widetilde{z})^*}{\overline{\rho}^*} \tag{3.21}$$

$$\frac{1}{\overline{\rho}^*} = \int_0^1 \frac{1}{\rho(z)}\widetilde{P}^*(z)dz \tag{3.22}$$

The corrected velocity field is computed at the corrector step

$$(\overline{\rho}\widetilde{u}_i)^* = \widehat{(\overline{\rho}\widetilde{u}_i)^*} - \Delta t^n \frac{\partial \overline{p}^*}{\partial x_i} \tag{3.23}$$

where the pressure is obtained solving the Poisson equation

$$\frac{\partial \widehat{(\overline{\rho}\widetilde{u}_i)^*}}{\partial x_i} + \frac{\partial \overline{\rho}^*}{\partial t} = \Delta t^n \frac{\partial^2 \overline{p}^*}{\partial x_i \partial x_i} \tag{3.24}$$

where the time derivative of the density is obtained as

$$\frac{\partial \overline{\rho}^*}{\partial t} = (\frac{2\Delta t^n + \Delta t^{n-1}}{\Delta t^n(\Delta t^n + \Delta t^{n-1})})\overline{\rho}^* - (\frac{\Delta t^n + \Delta t^{n-1}}{\Delta t^n \Delta t^{n-1}})\overline{\rho}^n + (\frac{\Delta t^n}{\Delta t^{n-1}(\Delta t^n + \Delta t^{n-1})})\overline{\rho}^{n-1} \tag{3.25}$$

Corrector Step In the corrector step, applying the second order Adams-Moulton method to the Navier-Stokes system and to the mixture fraction equation, one obtains

$$\frac{\widehat{(\overline{\rho}\widetilde{u}_i)^{n+1}} - (\overline{\rho}\widetilde{u}_i)^n}{\Delta t^n} = \frac{1}{2}Res_u^n + \frac{1}{2}Res_u^{n-1} \tag{3.26}$$

$$\frac{(\overline{\rho}\widetilde{z})^{n+1} - (\overline{\rho}\widetilde{z})^n}{\Delta t^n} = \frac{1}{2}Res_z^n + \frac{1}{2}Res_z^{n-1} \tag{3.27}$$

From the known predicted mixture fraction field the density field is calculated as

$$\widetilde{z}^{n+1} = \frac{(\overline{\rho}\widetilde{z})^{n+1}}{\overline{\rho}^*} \tag{3.28}$$

$$\frac{1}{\overline{\rho}^{n+1}} = \int_0^1 \frac{1}{\rho(z)} \widetilde{P}^{n+1}(z)dz \tag{3.29}$$

The corrected velocity field is computed at the corrector step

$$(\overline{\rho}\widetilde{u}_i)^{n+1} = \widehat{(\overline{\rho}\widetilde{u}_i)^{n+1}} - \Delta t^n \frac{\partial \overline{p}^{n+1}}{\partial x_i} \tag{3.30}$$

The pressure is obtained solving the Poisson equation

$$\frac{\partial \widehat{(\overline{\rho}\widetilde{u}_i)^{n+1}}}{\partial x_i} + \frac{\partial \overline{\rho}^{n+1}}{\partial t} = \Delta t^n \frac{\partial^2 \overline{p}^{n+1}}{\partial x_i \partial x_i} \tag{3.31}$$

where the time derivative of the density is computed as

$$\begin{aligned} \frac{\partial \overline{\rho}^{n+1}}{\partial t} &= \left(\frac{2\Delta t^n + \Delta t^{n-1}}{\Delta t^n(\Delta t^n + \Delta t^{n-1})}\right)\overline{\rho}^{n+1} \\ &- \left(\frac{\Delta t^n + \Delta t^{n-1}}{\Delta t^n \Delta t^{n-1}}\right)\overline{\rho}^{n} \\ &+ \left(\frac{\Delta t^n}{\Delta t^{n-1}(\Delta t^n + \Delta t^{n-1})}\right)\overline{\rho}^{n-1} \end{aligned} \tag{3.32}$$

3.2 CMC Solver

The CMC code used in this research has been developed at the university of Cambridge [25]. In the CMC code, spatial terms in the CMC equations are discretized on a rectangular grid via a finite difference approach. A second order central scheme is used for discretizing the diffusion terms whereas the convective terms are discretized with a first order upwind scheme. To calculate the chemical reaction rates, the CHEMKIN II package is used. The resultant set of ODEs are integrated in time using the VODPK package [3]. This integration is done in a segregated manner so that first the integration for convection-diffusion in space is done, next the integration for diffusion in mixture fraction sample space and finally the integration for the chemical source term. This segregated method, also called operator splitting, has advantage over the method of lines. The advantage of this segregated solution procedure is less computational time for solving the set of CMC equations.

4 Test Case Description

Delft flame III, a non-premixed piloted flame, is a suitable test case for validation of turbulent combustion models due to its low Reynolds number yet strong interaction between chemistry and turbulence. The test case was studied experimentally by Delft University [16] and [24]. The fuel jet in this case is Dutch natural gas which is a mixture of 81.29% CH_4, 2.87% C_2H_6, 0.38% C_3H_8, 0.15% C_4H_{10}, 0.04% C_5H_{12}, 0.05% C_6H_{14}, 14.32% N_2, 0.01% O_2 and 0.89% CO_2. For the simulation, the fuel mixture is replaced by 85.3% CH_4 and 14.7% N_2 by volume. To avoid flame lift off, 12 pilot flames, emerging from small separate holes (diameter 0.5 mm), positioned on a circle with radius 3.5 mm, are supplied. The pilot is a pre-mixture of C_2H_2, H_2 and air. The thermal power of the pilot is 200 W which is 1% of the total flame thermal power. The Reynolds number based on jet diameter and jet bulk velocity is 9700. The jet bulk velocity is $U_j = 21.9m/s$ which emanates from a nozzle with diameter of $D = 6mm$. The annulus flow of air which encloses the fuel jet and the pilot enters the domain with a bulk speed of 4.4 m/s. The whole burner is surrounded by a coflow of air at 0.4 m/s.

The mixture fraction is defined according to Bilger's formula [1] and is 1 in the fuel stream and 0 in the air stream.

$$\xi = \frac{2\frac{Y_C - Y_{C,o}}{W_C} + \frac{Y_H - Y_{H,o}}{2W_H} - \frac{Y_O - Y_{O,o}}{W_O}}{2\frac{Y_{C,f} - Y_{C,o}}{W_C} + \frac{Y_{H,f} - Y_{H,o}}{2W_H} - \frac{Y_{O,f} - Y_{O,o}}{W_O}} \tag{4.33}$$

The test case was studied numerically by Merci et al. [12] using transported scalar PDF and $k-\varepsilon$ RANS turbulence model. Roekaerts et al. [19] compared a scalar PDF and a velocity-scalar PDF approach also within a RANS context. Merci et al. [12] adopted different micromixing models in the transported scalar PDF. The present research focus on the numerical study of the Delft flame III combining large eddy simulation and conditional moment closure.

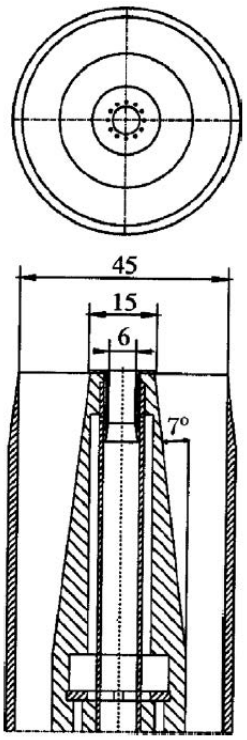

Figure 1: Schematic of Delft III burner

5 Results

For the simulation of Delft flame III, a cubic domain with a dimension of 50D in streamwise direction and 10D in lateral directions is used, where D is the nozzle diameter. The generated mesh consists of $144 \times 80 \times 80$ cells which are clustered towards the nozzle in all three physical dimensions. The CMC grid is much coarser: $15 \times 5 \times 5$ mesh points are used in physical space to discretize CMC equations. For discretizing the diffusion term of the CMC equations in mixture fraction sample space, 51 points are used. These points are clustered around the stoichiometric mixture fraction point which is 0.07 for Delft flame III. Finally for parallel computations, the domain is subdivided into 3 blocks. The computations were performed on a cluster of Xeon CPU. The LES code benefits from a variable time stepping approach [17] that helps to use the maximum allowed time step in each iteration. Simulations were done for approximately 20 flow through time based on jet bulk velocity and domain length. 10 flow through time which is equals to 0.015 second real time of flow simulation were performed to reach to statistically stationary state and then another 10 flow through time is performed for averaging. In total 15000 of sample were taken to compute the time averaged values.

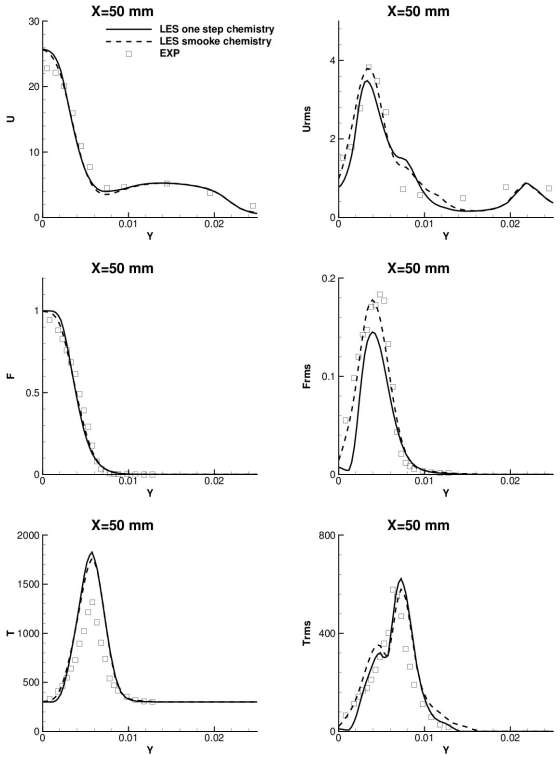

Figure 2: Radial profile of axial velocity, mixture fraction, temperature and their rms values at X=50 mm from the nozzle

To study the effect of the chemistry, two different methane reaction mechanisms are used. The first reaction mechanism is the one-step methane chemistry which was introduced by Fernandez-Tarrazo et al. [8]. The mechanism consist of only major species like CH_4, O_2, H_2O and CO_2. The second reaction mechanism is the Smooke reaction mechanism [23] which consists of 16 species and 25 reactions. The Smooke mechanism includes all major species plus intermediate and minor species like CO.

Results are shown in figures 2-6 for five different cross section. As can be seen in the figures 2-6, the axial velocity is predicted very well especially at $X = 50mm$ and $X = 100mm$ but as the flame emerge further downstream the predicted velocity decays faster than the experimental mea-

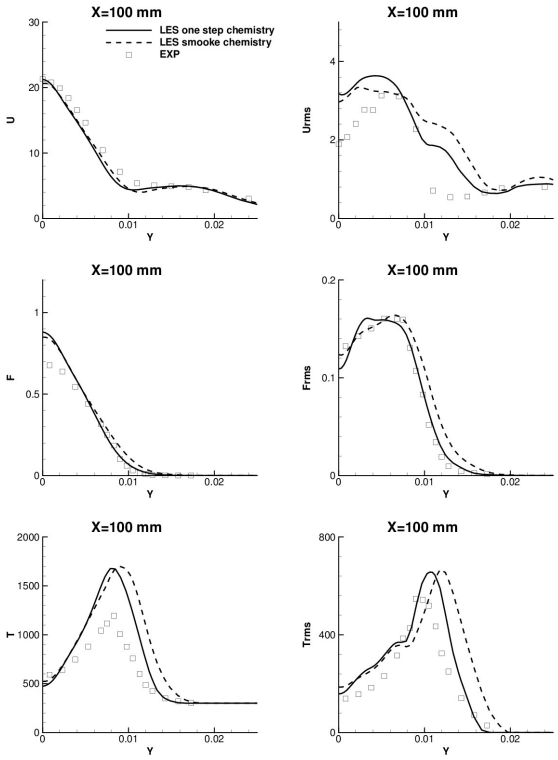

Figure 3: Radial profile of axial velocity, mixture fraction, temperature and their rms values at X=100 mm from the nozzle

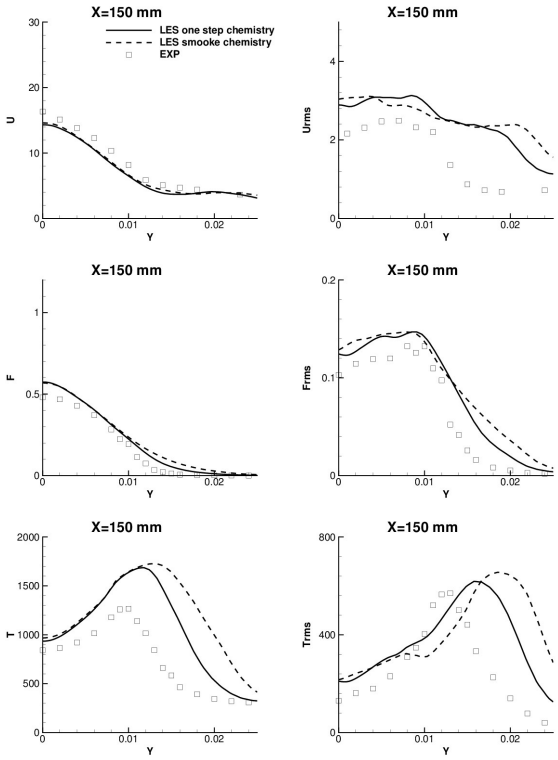

Figure 4: Radial profile of axial velocity, mixture fraction, temperature and their rms values at X=150 mm from the nozzle

surements. There is not much differences between predicted axial velocity of one step and Smooke chemistry.

The axial velocity rms is also shown in figures 2-6. It can be seen that the predicted rms value of axial velocity is in good agreement with experimental data especially in the locations where also the axial velocity is well predicted e.g. $X = 50mm$. Also it is seen that the rms value of axial velocity is predicted better with the Smooke chemistry than with one step chemistry.

The radial profile of the mixture fraction is also shown in figures 2-6. It can be seen that the predicted mixture fraction is in good agreement with the experiment close to the nozzle area, but it decays slower than experimental measurement further downstream. At $X = 200mm$ it is in good agreement but at $X = 250mm$ it is under-predicted. This behavior is related to the discretization of the convection term of the mixture fraction equation by TVD scheme. However, reaction mechanisms has no or little effects on predicted values of mixture fraction.

The rms values of the mixture fraction are also in good agreement with experimental data especially for areas close to the nozzle. It can be seen that for the Smooke chemistry the rms values of the mixture fraction is in better agreement with the experimental data than the one step chemistry especially close to nozzle area.

The temperature is also plotted in figures 2-6. It is obvious that the trend of the predicted temperature follows the measured values of the temperature. Also, the location of maximum temperature is predicted quite well. But there is an over-prediction of the temperature which can been seen in all cross section. As can be seen from the results, using more detailed chemistry has little effect on the prediction of the maximum temperature. But the Smooke mechanism can shift the location of maximum temperature and can affects the rms of temperature field quite drastically.

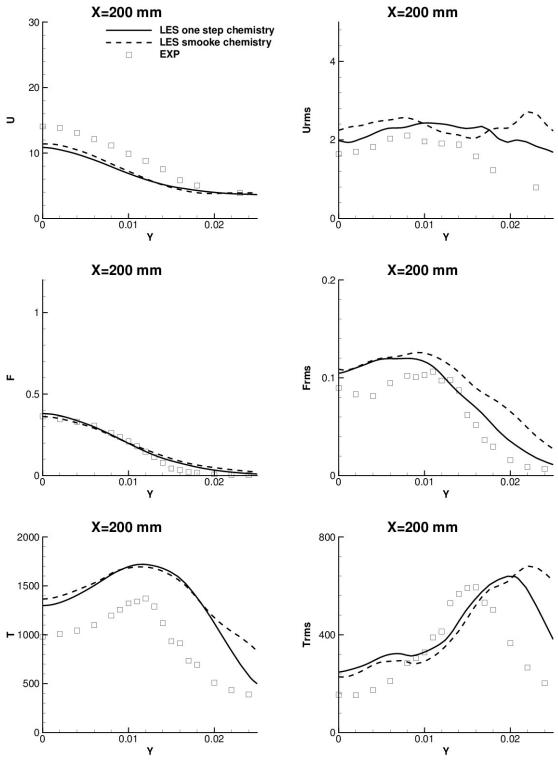

Figure 5: Radial profile of axial velocity, mixture fraction, temperature and their rms values at X=200 mm from the nozzle

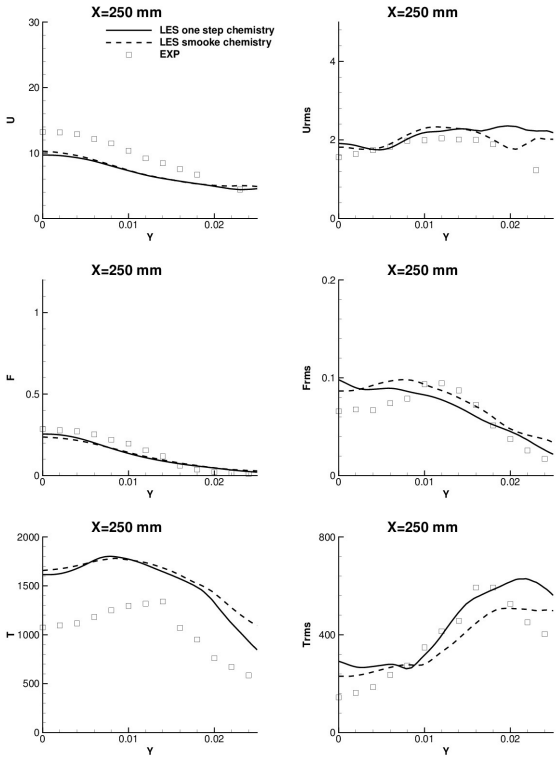

Figure 6: Radial profile of axial velocity, mixture fraction, temperature and their rms values at X=250 mm from the nozzle

6 Conclusions

Large eddy simulation of the Delft flame III is performed using a conditional moment closure approach. The fluid flow equations are solved using an in-house second order accurate finite volume code. The code uses a predictor-corrector time integration. A CMC code developed at the University of the Cambridge is used to solve the CMC equations. Two different reaction mechanisms are used to study the effects of the chemistry on the prediction of the flow as well as scalar fields. Results showed that using more detailed chemistry can lead to better prediction of rms values but has almost no influence on velocity and mixture fraction fields. Although the maximum temperature is insensitive to the chemistry model, the location that maximum temperature occurs is greatly influenced by different reaction mechanisms.

References

[1] R. W. Bilger, S. H. Starner, R. J. Kee, On reduced mechanisms for methane—air combustion in nonpremixed flame, *Combustion and Flame* 80 (1990) 135-149.

[2] N. Branley, W. P. Jones, Large eddy simulation of a turbulent non-premixed flame, *Combustion and Flame* 127 (2001) 1914-1934.

[3] P. N. Brown, G. D. Byrne, A. C. Hindmarsh, VODE, a variable-coefficient ODE solver, *SIAM Journal on Scientific Computing* 10 (1989) 1038-1051.

[4] C. M. Cha, G. Kosaly, H. Pitsch, Modeling extintion and reignition in turbulent nonpremixed combustion using a doubly-conditional moment closure approach, *Physics of Fluids* 13 (2001) 3824-3834.

[5] A. J. Chorin, Numerical solution of the Navier-Stokes equations, *Mathematics of Computation* 22 (1968) 745-762.

[6] M. Fairweather, R. M. Woolley, First-order conditional moment closure modeling of turbulent, nonpremixed hydrogen flames, *Combustion and Flame* 133 (2003) 393-405.

[7] M. Fairweather, R. M. Woolley, First-order conditional moment closure modeling of turbulent, nonpremixed methane flames, *Combustion and Flame* 138 (2004) 3-19.

[8] E. Fernandez-Tarrazo, A. L. Sanchez, A. Linan, F. A. Williams, A simple one-step chemistry model for partially premixed hydrocarbon combustion, *Combustion and Flame* 147 (2006) 32-38.

[9] S. S. Girimaji, Y. Zhou, Analysis and modeling of subgrid scalar mixing using numerical data, *Physics of Fluids* 8 (1996) 1224-1236.

[10] A. Kronenburg, Double conditioning of reactive scalar transport equations in turbulent nonpremixed flames, *Physics of Fluids* 16 (2004) 2640-2648.

[11] E. Mastorakos, R. W. Bilger, Second-order conditional moment closure for the autoignition of turbulent flows, *Physics of Fluids* 10 (1998) 1246-1248.

[12] B. Merci, D. Roekaerts, B. Naud, Study of the performance of three micromixing models in transported scalar PDF simulations of a piloted jet diffusion flame ("Delft flame III"), *Combustion and Flame* 144 (2006) 476-493.

[13] S. Navarro-Martinez, A. Kronenburg, F. di Mare, Conditional moment closure for large eddy simulation, *Flow, Turbulence and Combustion* 75 (2005) 245-274.

[14] S. Navarro-Martinez, A. Kronenburg, LES-CMC simulations of a turbulent bluff-body flame, *Proceedings of the Combustion Institute* 31 (2007) 1721-1728.

[15] S. Navarro-Martinez, A. Kronenburg, LES-CMC simulations of a lifted methane flame, *Proceedings of the Combustion Institute* 32 (2009) 1509-1516.

[16] T. W. J. Peeters, P. P. J. Stroomer, J. E. De Vries, D. J. E. M. Roekaerts, C. J. Hoogendoorn, Comparative experimental and numerical investigation of a piloted turbulent natural-gas diffusion flame, *Proceedings of the Combustion Institute* 25 (1994) 1241-1248.

[17] H. Pitsch, H. Steiner, Large-eddy simulation of a turbulent piloted methane/air diffusion flame (Sandia flame D), *Physics of Fluids* 12 (2000) 2541-2554.

[18] H. Pitsch, Large-eddy simulation of turbulent combustion, *Annual Review of Fluid Mechanics* 38 (2006) 453-482.

[19] D. Roekaerts, B. Merci, B. Naud, Comparison of transported scalar PDF and velocity-scalar PDF approaches to 'Delft flame III', *Comptes Rendus Mecanique* 334 (2006) 507-516.

[20] M. R. Roomina, R. W. Bilger, CMC predictions of a turbulent methane-air jet flame, *Combustion and Flame* 125 (2001) 1176-1195.

[21] M. R. H. Sheikhi, T. G. Drozda, P. Givi, F. A. Jaberi, S. B. Pope, Large eddy simulation of a turbulent nonpremixed piloted methane jet flame (Sandia flame D), *Proceedings of the Combustion Institute* 30 (2005) 549-556.

[22] J. Smagorinsky, General circulation experiments with the primitive equation, *Monthly Weather Review* 91 (1963) 99-165.

[23] M. Smooke, I. Puri, K. Seshadri, A comparison between numerical calculations and experimental measurements of the structure of a counterflow diffusion flame burning diluted methane in diluted air, *Twenty-First Symposium (International) on Combustion, The Combustion Institute, Pittsburgh* (1986) 1783-1792.

[24] E. H. van Veen, D. Roekaerts, On the accuracy of temperature measurements in turbulent jet diffusion flames by coherent anti-stokes raman spectroscopy, *Combustion Science and Technology* 175 (2003) 1893-1914.

[25] Y. M. Wright, G. de Paola, K. Boulouchos, E. Mastorakos, Simulations of spray autoignition and flame establishment with two-dimensional CMC, *Combustion and Flame* 143 (2005) 402-419.

Mahdi Zakyani Roudsari was born in 1979 in Tehran, Iran. He got his bachelor of science in mechanical engineering from University of Gilan in 2002. In 2005, he acquired his master of science in aerospace engineering from Sharif University of Technology. He managed to obtain his Ph.D. in mechanical engineering from Vrije Universiteit Brussel in Belgium in 2011. Dr Zakyani main research area focuses in the field of turbulent combustion and turbulence modeling of practical fluid dynamical systems. He currently works as faculty member at the Aerospace Research Institute (ARI). Mahdi Zakyani Roudsari is the corresponding author and can be contacted at: zakyani@ari.ac.ir